An Automated Matrix-Assisted Laser Desorption/Ionization Quadrupole Fourier Transform Ion Cyclotron Resonance Mass Spectrometer for "Bottom-Up" Proteomics

7 AUTHORS, INCLUDING:

Eric Peters

Genomics Institute of the Novartis Research …

80 PUBLICATIONS   6,184 CITATIONS

SEE PROFILE

Christopher M Shaw

Genomics Institute of the Novartis Research …

3 PUBLICATIONS   152 CITATIONS

SEE PROFILE

An Automated Matrix-Assisted Laser Desorption/ Ionization Quadrupole Fourier Transform Ion Cyclotron Resonance Mass Spectrometer for "Bottom-Up" Proteomics

Ansgar Brock,* David M. Horn, Eric C. Peters, Christopher M. Shaw, Christer Ericson, Qui T. Phung, and Arthur R. Salomon

Genomics Institute of the Novartis Research Foundation, 10675 John Jay Hopkins Drive, San Diego, California 92121

Here we describe a new quadrupole Fourier transform ion cyclotron resonance hybrid mass spectrometer equipped with an intermediate-pressure MALDI ion source and demonstrate its suitability for "bottom-up" proteomics. The integration of a high-speed MALDI sample stage, a quadrupole analyzer, and a FT-ICR mass spectrometer together with a novel software user interface allows this instrument to perform high-throughput proteomics experiments. A set of linearly encoded stages allows subsecond positioning of any location on a mircotiter-sized target with up to 1536 samples with micrometer precision in the source focus of the ion optics. Such precise control enables internal calibration for high mass accuracy MS and MS/MS spectra using separate calibrant and analyte regions on the target plate, avoiding ion suppression effects that would result from the spiking of calibrants into the sample. An elongated open cylindrical analyzer cell with trap plates allows trapping of ions from 1000 to 5000 m/z without notable mass discrimination. The instrument is highly sensitive, detecting less than 50 amol of angiotensin II and neurotensin in a μLC MALDI MS run under standard experimental conditions. The automated tandem MS of a reversed-phase separated bovine serum albumin digest demonstrated a successful identification for 27 peptides covering 45% of the sequence. An automated tandem MS experiment of a reversed-phase separated yeast cytosolic protein digest resulted in 226 identified peptides corresponding to 111 different proteins from 799 MS/MS attempts. The benefits of accurate mass measurements for data validation for such experiments are discussed.

In the last several years, mass spectrometry (MS) has become the leading technology for the characterization of complex protein mixtures. The development of "soft" ionization techniques such as electrospray ionization[1] and matrix-assisted laser desorption/ionization (MALDI)[2,3] in combination with database searching for protein identification[4,5] has brought about an explosion of new applications for protein analysis. Currently, intense research efforts focus on the high-throughput identification and quantitation of the full complement of expressed proteins (the "proteome") from a given biological sample, which is a major challenge due to the thousands of proteins per sample, the wide range of protein expression levels, and the numerous posttranslational modifications that can be found on any given protein. The most commonly used approach for such analyses employs two-dimensional gel electrophoresis (2DGE) separation of the intact proteins, excision of gel spots, tryptic digestion of the excised protein(s), and protein identification using peptide mass fingerprinting[4] or tandem mass spectrometry (MS/MS).[5] However, there are significant drawbacks to the use of 2DGE, most notably the limited dynamic range, throughput, and difficulty in characterizing proteins of high hydrophobicity, low abundance, or extreme p*I*. Thus, there is a significant effort to devise complementary methods to 2DGE for complex protein mixture analysis.

The most common alternative to the classic 2DGE strategy has been termed "gel-free" or "shotgun" proteomics. These methods typically directly couple single[6,7] or multidimensional[8,9] liquid separations to a mass spectrometer through an electrospray interface, performing data-dependent tandem MS to identify proteins. These technologies have been shown to identify low-abundance proteins in complex mixtures that are not typically detected using 2DGE-based technology[10] and can identify large numbers of proteins in organisms in a single experiment.[8] The major drawback with such an approach for comprehensive analysis is the time scale incompatibility between the separation and mass spectrometer, resulting in an upper limit to the number of analytes that can be identified based on the amount of time required for

---

(1) Fenn, J. B.; Mann, M.; Meng, C. K.; Wong, S. F.; Whitehouse, C. M. *Science* **1989**, *246*, 64−71.

(2) Karas, M.; Bachmann, D.; Bahr, U.; Hillenkamp, F. *Int. J. Mass Spectrom. Ion Processes* **1987**, *78*, 53−68.

(3) Karas, M.; Hillenkamp, F. *Anal. Chem.* **1988**, *60*, 2299−2301.

(4) Henzel, W. J.; Billeci, T. M.; Stults, J. T.; Wong, S. C.; Grimley, C.; Watanabe, C. *Proc. Natl. Acad. Sci. U.S.A.* **1993**, *90*, 5011−5015.

(5) Eng, J. K.; McCormack, A. L.; Yates, J. R. I. *J. Am. Soc. Mass Spectrom.* **1994**, *5*, 976−989.

(6) Figeys, D.; Ducret, A.; Yates, J. R., 3rd; Aebersold, R. *Nat. Biotechnol.* **1996**, *14*, 1579−1583.

(7) Ducret, A.; Van Oostveen, I.; Eng, J. K.; Yates, J. R., 3rd; Aebersold, R. *Protein Sci.* **1998**, *7*, 706−719.

(8) Washburn, M. P.; Wolters, D.; Yates, J. R., 3rd. *Nat. Biotechnol.* **2001**, *19*, 242−247.

(9) Wolters, D. A.; Washburn, M. P.; Yates, J. R., 3rd. *Anal. Chem.* **2001**, *73*, 5683−5690.

(10) Gygi, S. P.; Corthals, G. L.; Zhang, Y.; Rochon, Y.; Aebersold, R. *Proc. Natl. Acad. Sci. U.S.A.* **2000**, *97*, 9390−9395.

---

each tandem MS experiment. For complex samples, dozens to hundreds of peptides may be eluting concurrently and only a small percentage of these are subjected to tandem MS. While this can be mediated by reanalysis of the sample using exclusion lists to prevent the same peptides being identified or by adding additional dimensions of separation, this requires consumption of additional sample and substantially reduces throughput.

To overcome such time scale incompatibility, a number of research groups have described off-line approaches that decouple the final dimension of separation from the mass spectrometer. The most common techniques involve deposition of either fractions[11−14] or a continuous trace[15−18] of eluent by various means onto a MALDI target. Because there is no time constraint imposed on the mass analysis of these targets by the separations, intelligent choices can be made for which peptides should be selected for fragmentation[19] and generally more tandem mass spectra will be acquired in a single $LC^n/MS/MS$ experiment than can be performed for on-line methods. While the off-line experiment may require more time than the corresponding on-line technique, the overall throughput defined as information gained per unit time can be expected to be similar or even larger.

The type of mass spectrometer employed in an off-line separation/MALDI approach is a critical issue. The optimal instrument should have the highest possible dynamic range considering that protein expression levels in mammalian cells are estimated to vary over 7−8 orders of magnitude and might reach 10^{12} in serum,[20] be sensitive enough to detect peptides from proteins that express as low as a single copy per cell (amol sensitivity for 10^8 cells), have sufficient mass accuracy for highly confident protein identification, be able to resolve the signals of up to hundreds of peptides that may be eluting concurrently from the final dimension of a multidimensional separation, and be automated and fast enough to be able to characterize the tens of thousands of peptides from complex protein digests from mouse or human cell lines.

Fourier transform ion cyclotron resonance (FT-ICR) MS demonstrates the best combination of the desired capabilities for such a proteomics platform: low-ppm mass accuracy,[21] sub-attomole sensitivity,[22−24] the ability to resolve in a single spectrum thousands of peptides[25] and over 10 000 components from a crude oil sample,[26] and a dynamic range of more than 1000 in single-scan mode, which is comparable to the best performance of other mass spectrometric techniques. However, FT-ICR MS is currently not widely applied in high-throughput proteomics applications, mainly due to insufficient automation in commercially available FT-ICR systems. Furthermore, most of the current proteomics applications involving FT-ICR MS use electrospray ionization and direct infusion methods.[27,28] On-line coupling of FT-ICR MS with separations has been found to be quite challenging, mostly due to the several second time scale required for the acquisition of each MS or MS/MS spectrum and the difficulty in adding internal calibrants in electrospray experiments. Thus, decoupling of the separation from the mass spectrometer is especially important using FT-ICR MS, and therefore, a MALDI approach should prove quite valuable.

Here, we describe the first fully automated high-throughput MALDI quadrupole (Q)FT-ICR hybrid mass spectrometry system with an intermediate-pressure MALDI ion source[29,30] and integrated quadrupole mass spectrometer for high-throughput analysis of complex protein mixtures. The MALDI source is equipped with motion tables that can position any location on a microtiter plate-sized MALDI target with micrometer precision in less than 1 s on the ion optical axis of the instrument. This capability enables internal calibration to be performed for all spectra by a gas-phase mixing scheme in the ion optics, resulting in less than 5 ppm absolute mass accuracy (<2 ppm rms) across the full mass range for MS and tandem MS spectra of complex mixtures. All functions required for MS, tandem MS, and calibration have been automated to allow MS-only acquisitions from up to 1536 samples to be performed automatically in under 4 h. Furthermore, several hundred to thousands of targeted tandem mass spectra can be performed following the analysis of a MS run in a fully automated fashion.

INSTRUMENTATION

A schematic of the instrument divided into MALDI ion source, selection quadrupole, external accumulation[31] hexapole (EAH), injection quadrupole, and analyzer cell is shown in Figure 1 with typical experimental parameters. A 9.4-T actively shielded super-conducting magnet (Bruker Daltonics, Billerica, MA) was used for all experiments.

MALDI Source. The sample stage of the ion source consists of two stepper motor-driven cross-roller tables (Series 80600CT,

(11) Ericson, C.; Phung, Q. T.; Horn, D. M.; Peters, E. C.; Fitchett, J. R.; Ficarro, S. B.; Salomon, A. R.; Brill, L. M.; Brock, A. *Anal. Chem.* **2003**, *75*, 2309−2315.
(12) Ekstrom, S.; Nilsson, J.; Helldin, G.; Laurell, T.; Marko-Varga, G. *Electrophoresis* **2001**, *22*, 3984−3992.
(13) Miliotis, T.; Kjellstrom, M. T.; Onnerfjord, P.; Nilsson, J.; Laurell, T.; Edholm, L. E.; Marco-Varga, G. *J. Chromatogr., A* **2000**, *886*, 99−110.
(14) Laurell, T.; Nilsson, J.; Marko-Varga, G. *J. Chromatogr., B* **2001**, *752*, 217−232.
(15) Preisler, J.; Hu, P.; Rejtar, T.; Moskovets, E.; Karger, B. L. *Anal. Chem.* **2002**, *74*, 17−25.
(16) Preisler, J.; Hu, P.; Rejtar, T.; Karger, B. L. *Anal. Chem.* **2000**, *72*, 4785−4795.
(17) Wall, D. B.; Berger, S. J.; Finch, J. W.; Cohen, S. A.; Richardson, K.; Chapman, R.; Drabble, D.; Brown, J.; Gostick, D. *Electrophoresis* **2002**, *23*, 3193−3204.
(18) Lou, X.; van Dongen, J. L. *J. Mass Spectrom.* **2000**, *35*, 1308−1312.
(19) Peters, E. C.; Brock, A.; Horn, D. M.; Phung, Q. T.; Ericson, C.; Salomon, A. R.; Ficarro, S. B.; Brill, L. M. *LCGC Eur.* **2002**, *15*, 423−428.
(20) Corthals, G. L.; Wasinger, V. C.; Hochstrasser, D. F.; Sanchez, J. C. *Electrophoresis* **2000**, *21*, 1104−1115.
(21) Bruce, J. E.; Anderson, G. A.; Wen, J.; Harkewicz, R.; Smith, R. D. *Anal. Chem.* **1999**, *71*, 2595−2599.
(22) Valaskovic, G. A.; Kelleher, N. L.; McLafferty, F. W. *Science* **1996**, *273*, 1199−1202.
(23) Belov, M. E.; Gorshkov, M. V.; Udseth, H. R.; Anderson, G. A.; Smith, R. D. *Anal. Chem.* **2000**, *72*, 2271−2279.
(24) Belov, M. E.; Nikolaev, E. N.; Anderson, G. A.; Udseth, H. R.; Conrads, T. P.; Veenstra, T. D.; Masselon, C. D.; Gorshkov, M. V.; Smith, R. D. *Anal. Chem.* **2001**, *73*, 253−261.
(25) Bergquist, J.; Palmblad, M.; Wetterhall, M.; Hakansson, P.; Markides, K. E. *Mass Spectrom. Rev.* **2002**, *21*, 2−15.
(26) Hughey, C. A.; Rodgers, R. P.; Marshall, A. G. *Anal. Chem.* **2002**, *74*, 4145−4149.
(27) Meng, F.; Cargile, B. J.; Patrie, S. M.; Johnson, J. R.; McLoughlin, S. M.; Kelleher, N. L. *Anal. Chem.* **2002**, *74*, 2923−2929.
(28) Pasa-Tolic, L.; Lipton, M. S.; Masselon, C. D.; Anderson, G. A.; Shen, Y.; Tolic, N.; Smith, R. D. *J. Mass Spectrom.* **2002**, *37*, 1185−1198.
(29) Loboda, A. V.; Krutchinsky, A. N.; Bromirski, M.; Ens, W.; Standing, K. G. *Rapid Commun. Mass Spectrom.* **2000**, *14*, 1047−1057.
(30) O'Connor, P. B.; Costello, C. E. *Rapid Commun. Mass Spectrom.* **2001**, *15*, 1862−1868.
(31) Senko, M. W.; Hendrickson, C. L.; Emmett, M. R.; Shi, S. D.-H.; Marshall, A. G. *J. Am. Soc. Mass Spectrom.* **1997**, *8*, 970−976.
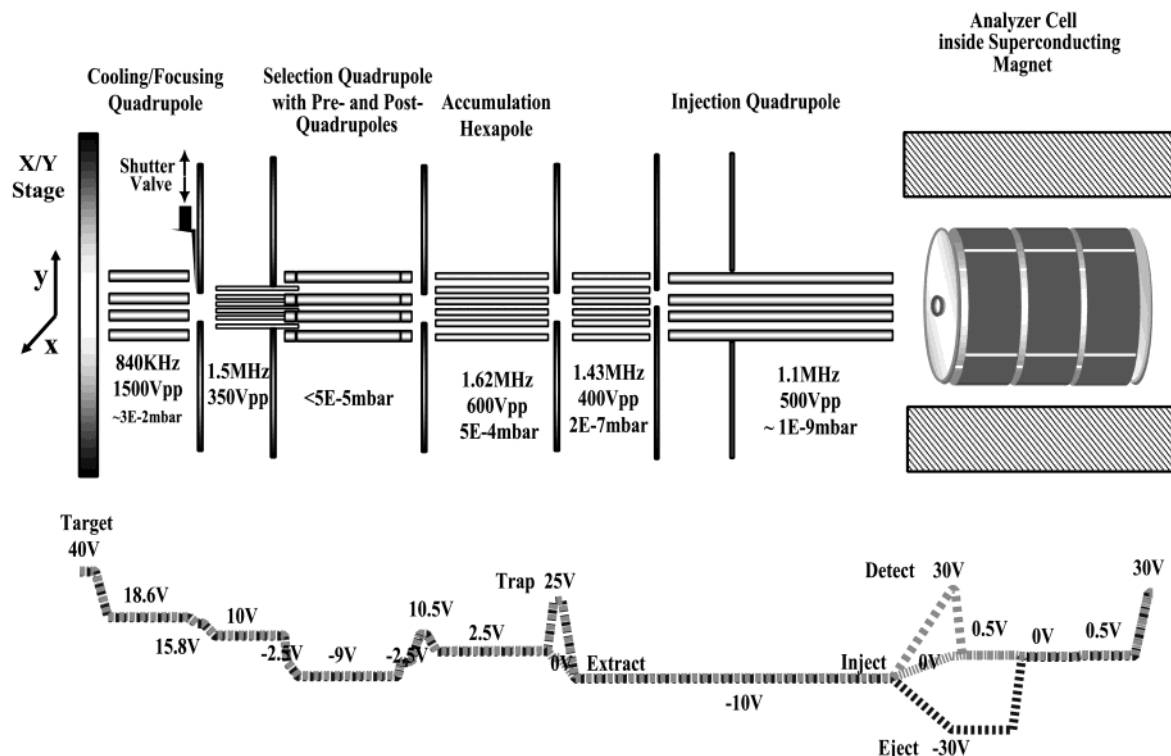
Figure 1. Schematic of QFT-ICR mass spectrometer ion optics with typical experimental conditions. At the bottom is a potential well diagram illustrating the applied dc potentials of the ion optics during the different stages of an experiment.

Parker-Hannifin Corp., Irvin, PA) mounted on top of each other for x- and y-coordinate addressability. The stepper motors are driven by independent amplifiers (GT-L5, Parker-Hannifin Corp.) controlled from a single two-axis controller (6K2, Parker-Hannifin Corp.). The stack of stages is mounted inside a custom-built source chamber ($550 \times 460 \times 200$ mm^3) evacuated by a molecular drag pump (MDP 5011, Alcatel, Hingham, MA) that is backed by a mechanical pump (E2M30, BOC Edwards, Wilmington, MA). The molecular drag pump is bypassed with a piece of $^1/_4$-in. tubing for accelerated pump down ($\sim$120 s) after target change. A shutter valve between the first quadrupole and subsequent hexapole allows the source chamber to be vented independently of the rest of the vacuum system, enabling rapid switching of MALDI targets. A needle valve is used to bleed dry nitrogen gas into the source and allows fine control over the static background pressure of the source chamber, which is generally kept at $\sim$(2–3) $\times$ 10^{-2} mbar. An additional ball valve allows rapid venting of the source chamber with dry nitrogen for rapid sample plate changes that take together with reevacuation of the chamber $\sim$3 min. Both stages are equipped with optical linear encoders that allow precise (1 μm) and fast (<1 s) positioning of any location on the sample plate underneath the focus of a 337-nm UV laser (VSL 337-ND-S, Laser Science, Franklin, MA). Microtiter plate-sized MALDI targets are mounted through an adaptor plate onto the stage stack, positioning the target 3 mm in front of the first quadrupole. The UV laser focus is positioned center to the first quadrupole and strikes the surface at an angle of $\sim$30° with respect to the surface normal. The beam from the external UV laser is guided to the source by two mirrors, one mounted outside and the other one inside the source chamber. A quartz lens with a focal length of 150 mm placed between the mirrors allows the laser fluence to

be adjusted by changing the size of the laser spot at the MALDI target. For the preferred MALDI matrix 2,5-dihydroxybenzoic acid (DHB), the strongest ion signal results when fluorescence emanating from a matrix-covered surface is observed from a roughly circular area with a diameter of 600 μm. These conditions allow the complete and uniform illumination of the 400-μm-diameter hydrophilic sample spots on the hydrophobic/hydrophilic targets.

Ion Optics. The ion optics train is composed of a sequence of multipole ion guides used for transmission, mass selection, and storage of ions. All multipoles except for the selection quadrupole were manufactured in-house. Typical voltages applied to these elements for ion accumulation and injection are given in Figure 1. Ions generated at the target surface after laser irradiation are collisionally cooled and guided toward the center of the first quadrupole (rod diameter, 9.5 mm; inscribed diameter, 8.2 mm; length, 138 mm) before being transmitted through a lens plate (orifice diameter, 3 mm) into a short hexapole ion guide (rod diameter, 1.6 mm; inscribed diameter, 3.2 mm, length, 54 mm) used to bridge excessive space in the second vacuum region. The bridging hexapole penetrates 3 mm through the entrance lens of a quadrupole assembly (QPS-4000, ABB Extrel, Pittsburgh, PA), which is powered and controlled by a quadrupole power supply (150-QC, ABB Extrel, Pittsburgh, PA). The pressure in this region is kept below 2 $\times$ 10^{-5} mbar by a turbomolecular pump (EXT255, BOC Edwards, Wilmington, MA). The exit lens plate of the quadrupole (orifice diameter, 3 mm) also serves as a conductance limit to the external ion accumulation region of the instrument consisting of a hexapole (rod diameter, 1.6 mm; inscribed diameter, 3.2 mm; length, 259 mm). The pressure in the accumulation region is adjusted to 5 $\times$ 10^{-4} mbar through nitrogen

bleeding. The two 3-mm-diameter conductance limits on either side of the chamber also serve as front and back trapping electrodes for the EAH. Three additional differentially pumped regions provide a pressure gradient that allows the UHV region of the analyzer to achieve a base pressure of 1×10^{-9} mbar (EXT501, BOC Edwards). The first of these differentially pumped chambers is bridged by a hexapole (rod diameter, 1.6 mm; inscribed diameter, 3.2 mm; length, 233 mm) and operates at 2×10^{-7} mbar (EXT501, BOC Edwards) during experiment execution. The adjacent region is separated by a conductance limit (diameter, 3 mm, pumped with EXT70, BOC Edwards) and the starting point of the injection quadrupole (rod diameter, 9.5 mm; inscribed diameter, 8.2 mm; length, 1324 mm), which protrudes through another conductance limit into the UHV region of the analyzer leaving a 5-mm gap between ion guide and cell entrance plate. With the exception of the selection quadrupole, homemade Q-head circuits employing resonant switch-mode excitation power all multipoles. Radio frequency oscillation of the drivers can be turned on and off by TTL triggers. Offset voltages for the rf elements are coupled with 10-MΩ resistors to the center taps of the rf-output coils of the Q-head circuits. Static dc voltages for the ion optics are supplied by a HV power supply (TD-9500, Spectrum Solutions, Russellton, PA). An electrospray controller (API 1600, Bruker Daltonics) supplies the "trap" and "extract" voltages on the plate behind the accumulation hexapole for external accumulation and ion injection.

Analyzer Cell. The analyzer cell is of a capacitively coupled open cylindrical design[32] equipped with additional front and back trap plates possessing 10-mm apertures for ion (front plate) and infrared laser beam (back plate) entry. The geometry is stretched compared to standard designs for increased charge capacity and improved gated trapping efficiency. The inner diameter of the three collinearly arranged cylinders forming the body of the cell is 65 mm, whereas the length of each cylinder is 85 mm. Each cylinder is split into quadrants spaced 3 mm apart. The cell segments and trap plates are held together by PEEK spacers that mount precisely into alignment holes on the outside of cell elements and trap plates. The center excite electrodes are capacitively coupled with 1-nF ceramic disk capacitors to the neighboring segments on the outer cylinders. Static dc bias voltages of typically 0.5 V are applied directly to the noncapacitively coupled outer segments and through 30-kΩ resistors to the capacitively coupled segments. The potentials on the trapping plates are varied between $+30$ and -30 V for gated trapping, detection, and clearing events of the cell by a cell controller (ICC, Bruker Daltonics). A relay is set up that transiently grounds the back cylinder of the cell to the rear trapping plate for the ion ejection steps described below.

Experimental Control. A schematic of the computers and controllers for the system is diagrammed in Figure 2. An APEX II acquisition console (Bruker Daltonics) is used for waveform generation, data acquisition, control of the cell voltages, and execution of TTL pulses that trigger MALDI stage movement and quadrupole selection during automated runs. XMASS 5.0 (Bruker Daltonics) is used to create experimental sequences, and its embedded Tcl/Tk scripting capabilities are used to provide a graphical user interface for the direct execution of commands from
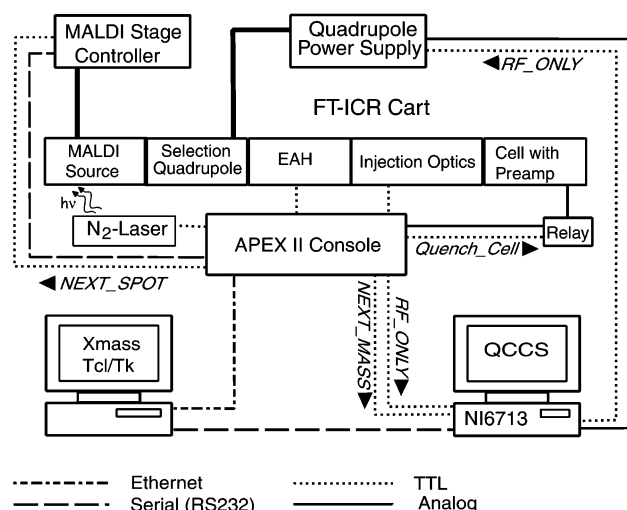
(32) Beu, S. C.; Laude, D. A. *Anal. Chem.* **1992**, *64*, 177−180.

Figure 2. Schematic of the components of the complete QFT-ICR MS system.

the host computer. Commands to the MALDI stage controller are transmitted from the host computer to the console through an ethernet connection and are subsequently transferred to the controller from the console using a serial connection. The selection quadrupole is controlled through a multifunction board (PCI6713, National Instruments, Austin, TX) residing in a second PC that runs the quadrupole communications and control software (QCCS, Figure 2) written in Microsoft Visual C++ and communicates with the host PC via serial communication. Software scripts residing on the MALDI stage controller, written with the help of supplied programming tools (Parker Compumotor Motion Planner, Parker-Hannifin Corp.), are used to govern manual and automatic movement of the stages and are triggered by a NEXT_SPOT TTL pulse from the acquisition console to go either to the calibrant strip or to the next target location in automated runs. For automated list acquisitions, the host computer sends the masses to be isolated by the quadrupole to the quadrupole control PC and the respective sample spot locations to the MALDI stage controller. The QCCS software is able to receive the trigger signals for NEXT_MASS and RF_ONLY from the acquisition console through the multifunction board. In response, the software instructs the quadrupole controller to switch between rf-only and mass selection mode and also supplies appropriate analog voltages to the quadrupole power supply to set the rf amplitude and dc offset voltages for mass selection.

Basic MS Event Sequence. After a target plate location is selected using either the custom-made Tcl/Tk tools to select a specific spot on a 96-, 384-, or 1536-well plate or the switches on the MALDI stage controller for manual selection, the user starts the run in XMASS. First, any leftover ions in the ion optics are ejected by applying a TTL pulse to the EAH Q-head that briefly stops oscillation, allowing the ions to escape. Any remaining ions in the cell are removed by transiently dropping the front plate and the elements of the first cylindrical electrode set to -30 V. Next, the laser is triggered to produce sample ions from the target, which travel along the potential gradient shown in Figure 1 to the EAH and are trapped in its potential well by collisional cooling with the background gas. Next, a valve is opened to raise the pressure in the UHV region to $\sim 2 \times 10^{-6}$ mbar of argon. The ion

injection optics are turned on, and the potentials of the cell front trap electrode and the first cylindrical electrode are set to 0 and 0.5 V, respectively. After a delay of 0.2 s, the back electrode of the EAH is lowered to 0 V, allowing the ions trapped in the EAH to travel into the cell through the injection optics. After another 3.5 ms, the front plate of the cell is raised to +30 V and the ion injection optics are turned off. Ions are allowed to cool in the elevated pressure of the UHV region for another 0.5 s before the argon gas flow is stopped. The high-vacuum region is allowed to pump down for $1-2$ s before excitation and detection. The total experiment time varies between 5 and 10 s.

Automated MS Event Sequence with Internal Calibration. The first step in an automated MS run is for the user to determine the spots to be analyzed and to move the stage to the target location of the first spot in the list using the customized Tcl/Tk tools. After the user starts the run, the leftover ions are ejected as before and the analytes from the spot are irradiated and stored in the EAH. The console then sends a TTL pulse (NEXT_SPOT) to trigger the MALDI stage to move to the closest of two calibrant strips located on the sides of the MALDI target. This strip is then UV-irradiated, and the ionized calibrants are transferred to the EAH where they mix with the stored analyte ions. The analyte and calibrants are subsequently transferred to the cell together. This procedure is similar to previously published work by O'Connor and Costello,[33] but the calibrants are instead mixed in the ion optics rather than the cell, resulting in significantly increased efficiency in the gas-phase mixing of the calibrant and analyte ions. Further, there is no requirement of samples being next to each other or in close proximity due to the speed of the sample stage, which allows much higher sample densities on the target plate and avoids the risk of cross-contamination during application of the calibrant. After the spectrum is acquired, the console sends another NEXT_SPOT TTL pulse to the MALDI stage controller to move from the calibrant strip to the next spot to be analyzed. These steps repeat until all spots are analyzed. All spectra are single scans, and since each experiment takes $5-10$ s, a 384-spot automated MS run can be analyzed in roughly 1 h.

Automated Tandem MS with Internal Calibration. The tandem MS experiment requires a text file that contains a list of target locations and m/z values denoting the analytes to be fragmented. The list of target locations is sent to the MALDI stage controller and stored in memory, while the list of masses is sent to the QCCS. The MALDI stage controller automatically moves the stage so that the first target location in the list is under the laser focus.

The experimental sequence is similar to the automated MS method with a few extra TTL pulses to control the ion selection. First, a TTL pulse (NEXT_MASS) is sent to the QCCS to set the quadrupole to select for the next mass in the list. Ions are removed from the ion optics and cell as before, but when the first analytes are being injected into the ion optics, the quadrupole only transmits ions within a $\sim$5 m/z wide window centered around the chosen mass. Prior to the injection of the calibrants, the RF_ONLY TTL pulse is sent to the QCCS to switch from mass-selective mode back to rf-only mode so that all of the calibrants travel to the EAH. After the ions are transferred to the cell, sustained off-resonance irradiation-collisionally activated dissocia-

tion (SORI-CAD)[34] is used to fragment the ions. The typical parameters for SORI are 0.5-s pulse duration, -1000-Hz frequency offset, and 28-dB attenuation. The NEXT_SPOT TTL pulse is sent to the MALDI stage controller to move to the next spot in the list. These steps repeat automatically until a tandem MS spectrum is recorded for all analytes in the submitted list. The acquisition of a tandem MS spectrum for each analyte requires roughly 10 s.

EXPERIMENTAL SECTION

Chemicals. HPLC grade solvents acetonitrile (MeCN), ethanol, methanol, hexane, and isopropyl alcohol (IPA) were purchased from Fisher (Pittsburgh, PA). Acetic acid, trifluoroacetic acid (TFA), N,N-dimethylformamide, poly(2-vinylpyridine) MW 4800 (PVP), DHB, α-cyano-4-hydroxycinnamic acid (HCCA), 6-aza-2-thiothymine (ATT), ammonium bicarbonate, 1,4-dithio-DL-threitol (DTT), and iodoacetamide (IAA) were supplied by Aldrich (St. Louis, MO). Formic acid was purchased from Riedel-de Haën (Seelze, Germany). Ammonium citrate dibasic (DAC) and urea were purchased from Sigma (St. Louis, MO). Deionized water (18 MΩ) was drawn from a water purification system (Nanopure Infinity, Barnstead/Thermolyne, Dubuque, IO). The 1536-spot target plates with 400-μm-diameter hydrophilic spots were obtained from Bruker Daltonics (AnchorChip) and cleaned according to the manufacturer's instructions before use. Grade 316 stainless steel balls of 2.4-mm diameter were purchased from Small Parts (NC9864467, Small Parts Inc., Miami Lakes, FL).

Matrix Purification. ATT was used without further purification. DHB and HCCA were recrystallized from equivolume mixtures of water and ethanol and air-dried.

Preparation of Calibrant Mixture. A total of 3 mg of PVP and 300 mg of ATT were dissolved in 15 mL of an equivolume mixture of IPA, formic acid, and water. One-milliliter aliquots of this solution were placed into individual centrifuge tubes and were dried in a SpeedVac vacuum evaporator (ThermoSavant, Holbrook, NY). To each tube, $3-4$ stainless steel balls and 500 μL of a nonpolar solvent such as hexane or methylene chloride were added to the dried crystals, and the tube was shaken using a vortex for several minutes at high speed to produce a fine slurry.

Preparation of Total Yeast Extracts from _Saccharomyces cerevisiae._ _S. cerevisiae_ (strain L40[35]) was grown to OD 600 of 2.7 in 500 mL of YPD media in a 2-L shake flask and incubated at 30 °C and 250 rpm. The cells were pelleted at 4000g, and the pellets were weighed after washing once with water. Cells were then incubated with shaking for 15 min at 30 °C in Tris$-$DTT buffer (0.1 M Tris, pH 9.4, 10 mM DTT). Subsequently, the cells were washed in buffer A (1.2 M sorbitol, 20 mM potassium phosphate, pH 7.4) and incubated for 30 min at 30 °C with shaking in 2 mL of buffer A/g of yeast pellet and Zymolyase 20T (ICN Pharmaceuticals, Costa Mesa, CA) at 2.5 mg/g of yeast pellet. The resulting spheroplasts were washed twice at 4 °C with buffer A by centrifugation at 4000g. Spheroplasts were then lysed in lysis buffer (50 mM Tris pH 7.5, 100 mM NaCl, 1% Nonidet P40, 20 μg/mL aprotinin, 20 μg/mL leupeptin, 1 mM Perfabloc, 10 mM β-glycerophosphate, 1 mM EDTA, and 10% glycerol (all from Sigma)) and cleared at 12000g for 15 min at 4 °C. Supernatant was stored at -80 °C at 10 mg/mL in lysis buffer.

(33) O'Connor, P. B.; Costello, C. E. _Anal. Chem._ **2000**, _72_, 5881$-$5885.

(34) Gauthier, J. W.; Trautman, T. R.; Jacobson, D. B. _Anal. Chim. Acta_ **1991**, _246_, 211$-$225.

(35) Vojtek, A. B.; Hollenberg, S. M.; Cooper, J. A. _Cell_ **1993**, _74_, 205$-$214.

Enzymatic Digestion. Protein solutions were first denatured in a solution of 100 mM ammonium bicarbonate and 8 M urea (pH 8.0) at 37 °C for 2 h. DTT was added to a final concentration of 0.01 M, and the solution was incubated at 60 °C for 2 h. After cooling to room temperature, the proteins were alkylated using IAA (final concentration of 0.02 M) for 20 min in the dark. The solution was subsequently diluted to 2 M urea, trypsin was added in a 1:40 (w:w) trypsin/analyte ratio, and the solution was allowed to digest overnight. The following morning, another equivalent aliquot of trypsin was added and the solution was incubated at 37 °C for an additional 4 h.

Deposition of Protein Digest Samples onto Target Plates. Samples were manually loaded onto a 15-cm-length, 300-μm PepMap column packed with 3-μm C-18 beads (LC Packings, Amsterdam, The Netherlands) using a syringe pump and washed for 10 min using solvent A (0.1% TFA) with an HP1100 capillary LC pump (Agilent, Palo Alto, CA) operated at a flow rate of 3 μL/min. Samples were separated using a gradient from 10 to 60% solvent B (0.1% TFA in MeCN) over 60 min and then 60−95% B over an additional 10 min. The postcolumn eluent was mixed with a DHB matrix solution (16 mg/mL DHB, 0.1 mg/mL DAC, 1% TFA), introduced using a syringe pump operating at 1 μL/min, in a low-volume Y connector (MY1XCS6, Vici Valco Instruments, Houston, TX). The mixed eluent and calibrant were subsequently deposited onto MALDI target plates in a raster pattern using a novel deposition device[11] in 5- (768 total fractions) or 10-s fractions (384 total fractions) onto target plates and were allowed to air-dry. Roughly 150 μL of the PVP internal calibrant slurry was evenly applied by pipet as two 3-mm-wide strips roughly 1 mm outside the first and last columns of sample on the MALDI target plate.

Data Reduction and Database Searching. To conserve disk space and minimize file transfer time, the 1 million-point time domain waveforms and the 32 000-point truncated Fourier transforms were stored directly to a server. Data reduction was carried out automatically with in-house-written software based on the THRASH algorithm.[36] Time domain waveforms were optionally apodized (Hanning) and zero-filled before computing the Fourier transform magnitude spectra. This was followed by automatic internal calibration, peak fitting, and removal of internal calibrant and known contaminant masses. For samples deposited during the course of a LC run, a procedure was invoked from within the software to combine signals that appear in spectra from consecutive spots, grouping the set of masses for the elution profile of each analyte as one entry in the new list. This reduced list was used to select which peptides masses should be submitted for tandem MS. Currently, this selection is performed manually, but software is currently being developed that creates lists of analytes for tandem MS based on user-determined criteria such as expression ratio or analyte abundance. For automated tandem MS experiments, the data were reduced automatically into a large file consisting of Mascot generic format lists of masses from each acquired tandem MS spectrum. The data were subsequently submitted to Mascot (Matrix Science, London, U.K.) directly or through Mascot Daemon for protein identification using 10 ppm tolerance on the parent ion, 30 mmu tolerance on the fragments,
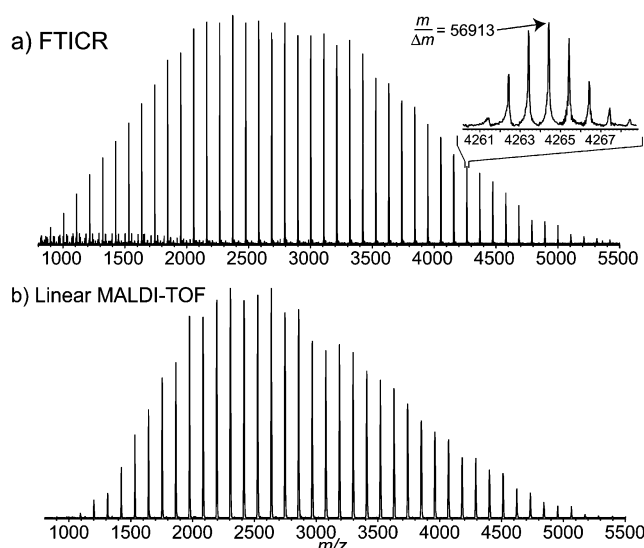

Figure 3. Mass spectrum of poly(vinylpyridine) recorded on (a) QFT-ICR mass spectrometer and (b) linear TOF mass spectrometer. The inset shows an expanded region of (a) around m/z 4264 revealing the resolution achieved at that m/z value.

and "semi-trypsin" specificity where at least one end of the peptide results from a standard tryptic cleavage. For assignment of the identities of tryptic peptides in a single protein, the protein sequence was directly loaded into PAWS (Genomics Solutions, Ann Arbor, MI) and masses were assigned to possible proteolytic peptides within 10 ppm.

Sensitivity Experiments. The 25 pM solutions of angiotensin and neurotensin were prepared in a 1 mg/mL BSA aqueous blocking buffer solution. Full loop injection of 2 μL of each solution onto a reversed-phase column was followed by chromatographic separation, automated deposition onto hydrophilic/hydrophobic sample plates,[37] and recrystallization as previously described[11,38] using HCCA as the matrix. Data were acquired as described above in the automated MS mode with 100 laser shots/spot but without internal calibration.

MALDI-TOF Data. The mass spectrum of poly(vinylpyridine) was obtained in linear mode on a Bruker Biflex III MALDI mass spectrometer.

RESULTS AND DISCUSSION

Trapping Characteristics. An initial area of concern was whether mass discrimination would be observed as a result of time-of-flight effects occurring during the ion transfer from the EAH to the analyzer cell. Mass spectra of PVP were acquired with ion-transfer times in the range 2.5−5.5 ms, with the spectrum for 3.5 ms shown in Figure 3a. There was no appreciable difference in the shapes of the distributions for the different flight times, but the signal was greatest for the 3.5-ms ion-transfer time setting. The absence of observable time-of-flight effects[39,40] may be due

(36) Horn, D. M.; Zubarev, R. A.; McLafferty, F. W. *J. Am. Soc. Mass Spectrom.* **2000**, *11*, 320−332.

(37) Schuerenberg, M.; Luebbert, C.; Eickhoff, H.; Kalkum, M.; Lehrach, H.; Nordhoff, E. *Anal. Chem.* **2000**, *72*, 3436−3442.

(38) Phung, Q. T.; Brock, A.; Horn, D. M.; Peters, E. C.; Ericson, C., Orlando, Fl, American Society for Mass Spectrometry, June 2−6, 2002.

(39) O'Connor, P. B.; Duursma, M. C.; van Rooij, G. J.; Heeren, R. M. A.; Boon, J. J. *Anal. Chem.* **1997**, *69*, 2751−2755.

(40) Easterling, M. L.; Mize, T. H.; Amster, I. J. *Int. J. Mass Spectrom. Ion Processes* **1997**, *169/170*, 387−400.

Table 1. Characteristic Experimental and Theoretical Values for Selected Peaks from the Spectrum Shown in Figure 3a

oligomer	most abundant m/z		ppm error	S/N	resolution	
	exptl	theoret			exptl	theoret[a]
12-mer	1320.7834	1320.7828	−0.4	762	137542	194942
16-mer	1741.0137	1741.0142	0.3	1410	131459	147888
20-mer	2161.2452	2161.2456	0.2	1954	107092	119133
24-mer	2582.479	2582.4801	0.4	1985	94361	99701
28-mer	3002.7121	3002.7115	−0.2	1901	82262	85748
32-mer	3422.94262	3422.9429	0.1	1679	67524	75220
36-mer	3844.1833	3844.1774	−1.5	1161	63049	66978
40-mer	4264.41379	4264.4088	−1.2	722	56913	60378

[a] Calculated for magnitude mode spectrum with a detection time of 2.15 s.

to the elongated cell, which can compensate for the spatial spread of the ions having different m/z values and kinetic energies.

The mass spectrum of the PVP calibrant mixture was also acquired on a MALDI TOF in linear mode (Figure 3b). As seen in the figure, the shapes of the distributions from the two instruments are similar. However, a significant effect on the shape of the distribution was seen when the attenuation of the excitation waveform was changed. A decrease in the attenuation by 2 dB from the value used in Figure 3a caused a 400 m/z shift in the maximum of the distribution (data not shown). This is likely due to the distortion of the excitation waveform generated by the Apex II acquisition console during amplification and coupling to the excitation electrodes. The excitation power seems to exhibit a negative slope across the full m/z range. For lower power excitations, the lower m/z oligomers are excited closer to the detection plates than those of higher m/z, increasing their signal. For higher power excitations, the lower m/z oligomers are excited to a radius where their cyclotron motion becomes unstable and their signals decay faster than the higher m/z oligomers. This problem may be solved by implementing an excitation method that enables a customizable excitation profile such as SWIFT.[41]

Resolution. FT-ICR is known for its exemplary resolution, but resolution does degrade with increasing m/z in a broadband spectrum.[42] The inset in Figure 3a shows that the FT-ICR easily resolves the isotopic cluster of the 40-mer of PVP at m/z 4264, with an observed resolution of 56 913 (see Table 1). This value is very close to the low-pressure limit theoretical resolution of 60 378 for an acquisition time of 2.15 s.[42] The resolutions for selected isotopic clusters from the spectrum in Figure 3a range from 50 000 to 150 000 as shown in Table 1. The lowest m/z isotopic cluster in the list, the 12-mer of polyvinylpyridine, shows by far the largest deviation from the theoretical limit, likely due to the uneven excitation waveform described above that causes the signal for this cluster to decay faster than the higher m/z clusters. This was confirmed by truncating the data to 512K points, resulting in a resolution of the 12-mer of 91 262, which is much closer to the theoretical limit of 97 471. Thus, the signal for the 12-mer does strongly decay after the first ~1 s of the waveform, while the

signals for the remaining isotopic clusters have not decayed significantly over the original 2.15-s acquisition time.

Mass Accuracy. The single-scan PVP spectrum obtained by the MALDI FT-ICR was internally calibrated using the most abundant peaks from every fourth isotopic cluster from m/z 1109 (12-mer) to 4474 (40-mer). After calibration, the most abundant m/z values were calculated for oligomers between the calibrants (Table 1). For peaks below m/z 3500, all of the masses were within 0.5 ppm of the expected value, while the two higher m/z oligomers were within 1.5 ppm. Given both the total number of peaks observed and the fact that the more abundant isotopic clusters exhibit signal-to-noise ratios of nearly 2000, significantly larger space charge-induced mass errors would be expected. The considerable charge capacity of the elongated cell and the high magnetic field presumably mitigate the space charge effects so that high mass measurement accuracy is maintained even under nonideal conditions.

This high mass accuracy over such a large m/z range makes it feasible to use an accurate mass approach for protein identification, in which a protein from a sample is identified from the mass of only one of its proteolytic peptides and potential compositional information for that peptide.[43] Preliminary results[44] have shown that proteins can be identified in this manner from the organism *Thermotoga maritima* using accurate mass measurement with additional compositional information gleaned from the use of an isotopically labeled lysine-specific reagent.[19] Accurate mass measurement identifications would dramatically increase the throughput of protein identification in complex mixtures by decreasing the number of required tandem MS experiments.

Sensitivity. Mass spectra of samples containing less than 50 amol each of peptides angiotensin II and neurotensin are shown in Figure 4. Despite performing full reversed-phase separation that resulted in each peptide being distributed into several fractions on the sample plate, both peptides could still be detected in two sample locations. The amount of sample actually detected in each spectrum is much lower than the total of 50 amol injected due to the signal splitting for each peptide as well as the unavoidable sample losses during the processing steps. With modifications to the ion ejection optics of the EAH similar to that described by Wilcox et al.,[45] it is conceivable that zeptomole sensitivity could be achieved on this instrument, as has been obtained for multiply charged ions on electrospray FT-ICR instruments.[22−24]

MALDI Automation. Although TOF analyzers can be used to automatically collect mass spectra for multiple samples on a MALDI target plate, there are several drawbacks to their use in such applications. First, the number of ions produced per laser shot needs to be tightly controlled in order to avoid exceeding the dynamic range of the detection systems. Further, space charge, geometrical, and energetic effects in the source region of MALDI TOF instruments can cause severe signal degradation. Therefore, laser intensity is typically set just above threshold and ions are produced from rather small areas of a sample.[46] However, commonly used MALDI matrixes such as DHB exhibit "sweet

(41) Chen, L.; Wang, T. C.; Ricca, T. L.; Marshall, A. G. *Anal. Chem.* **1987**, *59*, 449−454.

(42) Marshall, A. G.; Hendrickson, C. L.; Jackson, G. S. *Mass Spectrom. Rev.* **1998**, *17*, 1−35.

(43) Conrads, T. P.; Anderson, G. A.; Veenstra, T. D.; Pasa-Tolic, L.; Smith, R. D. *Anal. Chem.* **2000**, *72*, 3349−3354.

(44) Horn, D. M.; Brock, A.; Peters, E. C.; Ericson, C.; Ficarro, S. B.; Phung, Q. T.; Salomon, A. R.; Shaw, C. M. *Proc. Am. Soc. Mass Spectrom. Conf.*, Orlando, FL, 2002.

(45) Wilcox, B. E.; Hendrickson, C. L.; Marshall, A. G. *J. Am. Soc. Mass Spectrom.* **2002**, *13*, 1304−1312.
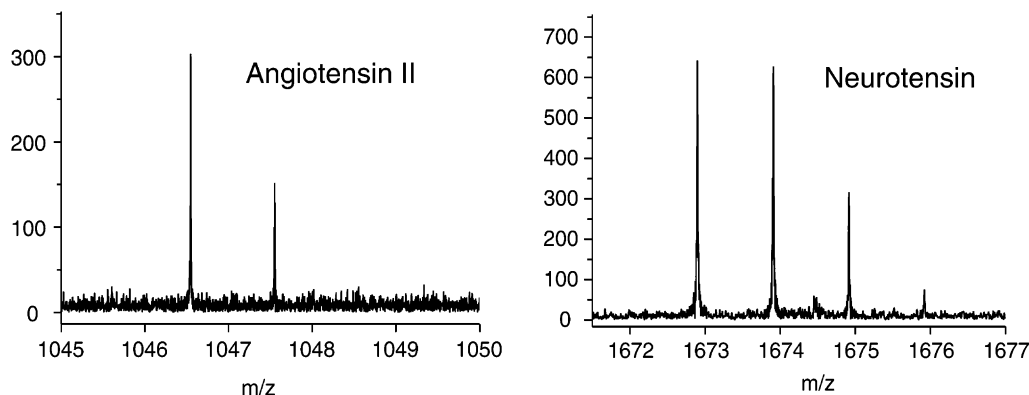
Figure 4. Signals detected by the MALDI QFT-ICR mass spectrometer for angiotensin II and neurotensin at the peak of their elution profiles from a reversed-phase LC separation deposited onto a MALDI target.

spots" due to sample heterogeneity of matrix/analyte cocrystallizates. Automation of the data acquisition process therefore requires extensive sampling at different locations as well as laser power attenuations to produce optimal data, which is a time-consuming process even if expert systems are employed.[46] Thus, matrixes producing more uniform signal are preferred,[47] leading to the prevalent use of HCCA in peptide work despite the fact that better signals and sequence coverages are obtainable with DHB.[48]

In contrast, automation on this new MALDI FT-ICR is achieved by concentration of the sample into an area small enough such that the whole spot can be illuminated at a laser power that maximizes ion production per shot but is low enough to avoid fragmentation. The buffer gas in the source provides collisional cooling[49] that minimizes ion fragmentation even at high laser powers and also reduces the initial kinetic energy of the ions, enabling efficient accumulation in the EAH and transfer to the cell. This combination results in robust automation without the need for expert systems to control the acquisition process. The advantages of intermediate-pressure MALDI for automation have been recognized early on in the development of orthogonal acceleration MALDI TOF MS instrumentation.[49] While acquiring a single MS spectrum on the MALDI TOF with a laser repetition rate of 10 Hz can require several minutes to obtain an optimized spectrum, the FT-ICR requires only 5−10 s/spot and still produces far superior data (manuscript in preparation).

MS/MS Performance. The two basic experiments performed for protein identification, peptide mass fingerpriting and tandem mass spectrometry, rely on the cross-correlation of mass spectral data with in silico digested or fragmented databases.[4,5] It is well recognized that the confidence of an assignment in either method increases dramatically with better mass accuracy.[50−55] While

peptide mapping is preferentially performed on an instrument equipped with a MALDI source, there are drawbacks to using such a source for tandem MS experiments. Singly charged ions demonstrate strong sequence-dependent fragmentation[56] and often yield limited sequence information especially for peptides that contain acidic amino acids. When performing database searches with limited sequence information, it is highly advantageous to have high mass accuracy measurements of both the parent ions and the fragments in order to greatly limit the number of possible matches. As such, a high mass accuracy analyzer would appear to be especially useful in conjunction with a MALDI-based approach for protein identification using tandem MS.

A reversed-phase separation of 1 pmol of a BSA tryptic digest was used as an initial test of the quality of internally calibrated automated MS/MS. The separation was deposited in 10-s fractions with matrix onto the 384 spots of a hydrophobic/hydrophilic target. The masses obtained from the MS run were tentatively assigned to predicted BSA tryptic peptides, and a list of the 76 possible peptide assignments within 10 ppm and their target locations was created for automated tandem MS. Even though absolute mass measurement accuracy is routinely below 5 ppm across the full mass range, 10 ppm was used here and in database searches to account for highly abundant analytes that exhibit larger mass errors due to peak-coalescence.[57,58] After automated tandem MS, the data were submitted to Mascot, which returned a score of 538 based on 27 total peptides identified by MS/MS covering 45% of the sequence of BSA. Surprisingly, three of the assigned peptides had a pyroglutamic acid modification and two showed oxidized methionines and thus did not correspond to the sequences that were originally assigned by PAWS. From these data, 35% of the attempted tandem MS experiments resulted in a confident identification of a peptide under the conditions used. It is likely that more peptides could be identified by the adjustment

(46) Jensen, O. N.; Mortensen, P.; Vorm, O.; Mann, M. *Anal. Chem.* **1997**, *69*, 1706−1714.

(47) Gobom, J.; Schuerenberg, M.; Mueller, M.; Theiss, D.; Lehrach, H.; Nordhoff, E. *Anal. Chem.* **2001**, *73*, 434−438.

(48) Unpublished results.

(49) Krutchinsky, A. N.; Loboda, A. V.; Spicer, V. L.; Dworschak, R.; Ens, W.; Standing, K. G. *Rapid Commun. Mass Spectrom.* **1998**, *12*, 508−518.

(50) Clauser, K. R.; Baker, P.; Burlingame, A. L. *Anal. Chem.* **1999**, *71*, 2871−2882.

(51) Zhang, W.; Chait, B. T. *Anal. Chem.* **2000**, *72*, 2482−2489.

(52) Perkins, D. N.; Pappin, D. J.; Creasy, D. M.; Cottrell, J. S. *Electrophoresis* **1999**, *20*, 3551−3567.

(53) Masselon, C.; Anderson, G. A.; Harkewicz, R.; Bruce, J. E.; Pasa-Tolic, L.; Smith, R. D. *Anal. Chem.* **2000**, *72*, 1918−1924.

(54) Goodlett, D. R.; Bruce, J. E.; Anderson, G. A.; Rist, B.; Pasa-Tolic, L.; Fiehn, O.; Smith, R. D.; Aebersold, R. *Anal. Chem.* **2000**, *72*, 1112−1118.

(55) Egelhofer, V.; Gobom, J.; Seitz, H.; Giavalisco, P.; Lehrach, H.; Nordhoff, E. *Anal. Chem.* **2002**, *74*, 1760−1771.

(56) Wattenberg, A.; Organ, A. J.; Schneider, K.; Tyldesley, R.; Bordoli, R.; Bateman, R. H. *J. Am. Soc. Mass Spectrom.* **2002**, *13*, 772−783.

(57) Marshall, A. G.; Hendrickson, C. L. *Int. J. Mass Spectrom.* **2002**, *215*, 59−75.

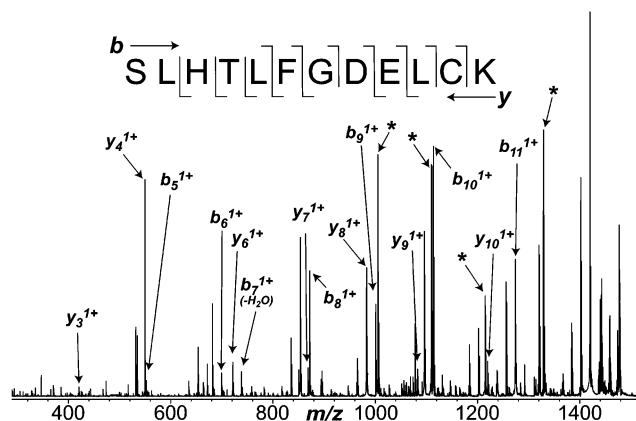(58) Naito, Y.; Inoue, M. *J. Mass. Spectrom. Soc. Jpn.* **1994**, *42*, 1−9.

Figure 5. Tandem MS spectrum of the peptide SLHTLFGDELCK of BSA with annotated b- and y-ion series (internal calibrant signals marked by *).

Figure 6. Tandem MS spectrum of NPVILADACCSR demonstrating the preferred cleavage at aspartic acid during SORI-CAD (internal calibrant signals marked by *).

of SORI-CAD conditions based on the m/z of the parent ion,[59] alternative fragmentation methods such as infrared multiphoton dissociation,[60] or the use of derivatization techniques to improve sequence coverage in tandem MS of singly charged ions.[52,61,62] In addition, a strategy using a parallel MS/MS approach[53] could easily be implemented with this instrument with a concomitant increase in throughput by 1 order of magnitude.

An exemplary tandem MS spectrum of the BSA peptide SLHTLFGDELCK is shown in Figure 5, which returned a Mascot score of 53. Significant b- and y-ion series and their respective water losses are observed. Mass accuracy in this case was somewhat limited because the internal calibrants did not extend below $m/z \sim 1000$ while fragments are observed down to m/z 400. However, the 5 ppm rms observed for these fragments still affords strong selectivity for protein identification.[52]

MS/MS of a Yeast Tryptic Digest. To test the instrument's performance under the more demanding conditions of complex mixture analysis, an automated LC tandem MALDI FT-ICR run was performed on a tryptic digest of yeast cytosolic proteins. The eluent of a reversed-phase separation of 10 μg of a yeast tryptic digest was deposited onto a hydrophobic/hydrophilic MALDI target, which resulted in well over 10 000 detected individual components.[19] From the MS data, 799 of the more abundant analytes (S/N > 30) were manually compiled into a list of their masses and target locations. After tandem MS, the resulting data were submitted to Mascot, leading to the identification of 226 peptides from 111 different yeast proteins, including ribosomal proteins, transcription initiation factors, heat shock proteins, and all of the enzymes involved in glycolysis (see Supporting Information for complete list). The tandem MS success rate of 28% (226/799) is actually rather high. Data-dependent tandem MS acquisitions on quadrupole ion trap mass spectrometers generally exhibit success rates for positive identifications of only 10% after validation.[28]
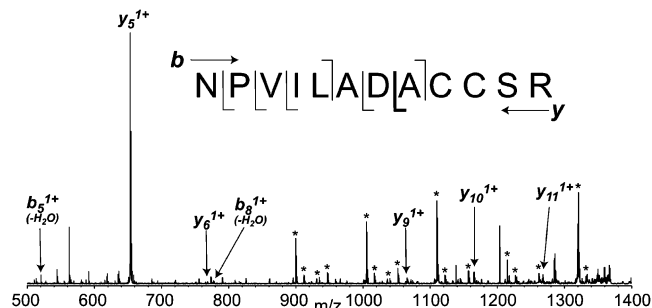
While the great majority of the identified peptides returned scores well below the Mascot calculated 95% confidence threshold of ~30−40 due to limited sequence information, the assignments were still unambiguous due to the high mass measurement accuracy. While there was often limited sequence information from the tandem MS because the precursor ions were singly charged, 182 of the 226 assigned peptides were assignable to only one peptide from the complete yeast proteome digested with "semi-trypsin" specificity (vide supra) because of the low-ppm accuracy of the precursor and fragment ions. These assignments were further strengthened by the knowledge that acidic amino acids strongly direct fragmentation for singly charged precursor ions.[63] For example, the tandem mass spectrum of a peptide from pyruvate decarboxylase that contained a single aspartic acid, NPVILADACCSR, shows a dominant y_5-fragment from backbone cleavage adjacent to the aspartic acid and only six other fragments of low abundance (Figure 6). Due to low sequence coverage, the resulting Mascot score of 10 for this peptide is well below the 95% confidence threshold of 35. However, the selectivity afforded by high mass measurement accuracy combined with the strong fragmentation expected adjacent to the aspartic acid restricts this as the only possible peptide from the proteome that fits the data.[63]

Another advantage of high mass measurement accuracy is the dramatic decrease in the amount of time required for the validation of tandem MS results. In our experience, data acquired during a reversed-phase μLC data-dependent experiment with instruments such as ion traps require several days to weeks of interpretation and validation. In contrast, high mass accuracy not only restricts assignment to one reasonable possibility in many cases but also results in very few misassigned peptides. Of the 799 submitted tandem mass spectra, Mascot returned potential assignments for only 257 species. Of these assignments, only 31 were rejected due to a variety of reasons, including unreasonable combinations of the variable modifications (e.g., multiple deamidations), the existence of only a small difference between the first and second best scores, peptides with no homology, and peptide assignments that do not exhibit strong fragmentation adjacent to their acidic amino acids. Furthermore, only five peptides were rejected with a score of over 6, so this value was empirically determined to be the 95% confidence level for Mascot. Since every score above 10 is almost certainly a correctly assigned peptide, only the data with

(59) Mirgorodskaya, E.; O'Connor, P. B.; Costello, C. E. *J. Am. Soc. Mass Spectrom.* **2002**, *13*, 318−324.

(60) Little, D. P.; Speir, J. P.; Senko, M. W.; O'Connor, P. B.; McLafferty, F. W. *Anal. Chem.* **1994**, *66*, 2809−2815.

(61) Munchbach, M.; Quadroni, M.; Miotto, G.; James, P. *Anal. Chem.* **2000**, *72*, 4047−4057.

(62) Keough, T.; Lacey, M. P.; Youngquist, R. S. *Rapid Commun. Mass Spectrom.* **2000**, *14*, 2348−2356.

(63) Sullivan, A. G.; Brancia, F. L.; Tyldesley, R.; Bateman, R.; Sidhu, K.; Hubbard, S. J.; Oliver, S. G.; Gaskell, S. J. *Int. J. Mass Spectrom.* **2001**, *210–211*, 665−676.

a score less than this must be verified. As a result, the complete validation of the tandem MS assignments for the reversed-phase run on the MALDI FT-ICR required only 30 min, which is significantly less than that required for similar experiments on quadrupole ion trap instruments.

The next step in this process is to increase the amount of sample loaded onto the system and to add another dimension of separation such as strong cation exchange. Using this instrument, a strong cation exchange/reversed-phase LC MS experiment of 200 μg of a yeast tryptic digest resulted in over 75 000 detected components.[44] It is expected that the dramatic increase in the number of signals observed will also result in a concomitant increase in the number of proteins identified.

CONCLUSIONS

It is widely known that high mass measurement accuracy is extremely beneficial in protein identification experiments. FT-ICR MS has consistently demonstrated low-ppm mass measurement accuracy, but it is often considered to lack robustness and requires significant expertise to operate. Furthermore, data-dependent tandem MS experiments with FT-ICR instruments in conjunction with on-line separation is difficult to implement due to the large amount of time required for any single tandem MS experiment. Thus, the widely utilized instruments (e.g., quadrupole ion trap, Q-TOF) for proteomics are generally less accurate instruments that are more easily automated and can obtain MS and tandem MS spectra very quickly. While a considerable amount of information is gained from these experiments, the resulting data are less reliable, leading to many days of grueling manual data validation.

In addition, any peptides that provide limited sequence information in tandem MS experiments will still remain unidentified by these instruments with lower mass accuracy, especially for organisms with a large proteome.

This article describes a MALDI QFT-ICR mass spectrometer designed specifically for high-throughput "bottom-up" proteomics that solves the incompatability of the time scale of the separation and the mass spectrometer while harnessing the power of high mass accuracy of FT-ICR MS. The off-line approach using microfraction collection and matrix-assisted laser desorption/ ionization in combination with other unique instrumental and operational factors allows the highly efficient automation of this instrument in both MS and MS/MS modes. Also, the utility of the high mass accuracy of this instrument is clearly demonstrated by the unambiguous identification of peptides that provide limited sequence information by tandem MS as well as the reduced amount of time for validation of automated tandem MS data.

SUPPORTING INFORMATION AVAILABLE

A tabulated summary of the 226-peptide identifications that resulted from automated LC tandem MALDI FT-ICR analysis of a yeast cytosolic protein digest. This material is available free of charge via the Internet at http://pubs.acs.org.